

ARTICLE

Received 2 Oct 2012 | Accepted 14 Mar 2013 | Published 23 Apr 2013

DOI: 10.1038/ncomms2753

Competing signals drive telencephalon diversity

J.B. Sylvester¹, C.A. Rich^{1,2}, C. Yi¹, J.N. Peres³, C. Houart³ & J.T. Strelman¹

The telencephalon is the most complex brain region, controlling communication, emotion, movement and memory. Its adult derivatives develop from the dorsal pallium and ventral subpallium. Despite knowledge of genes required in these territories, we do not understand how evolution has shaped telencephalon diversity. Here, using rock- and sand-dwelling cichlid fishes from Lake Malawi, we demonstrate that differences in strength and timing of opposing Hedgehog and Wingless signals establish evolutionary divergence in dorsal-ventral telencephalon patterning. Rock dwellers exhibit early, extensive Hedgehog activity in the ventral forebrain resulting in expression of *foxg1* before dorsal Wingless signals, and a larger subpallium. Sand dwellers show rapid deployment of Wingless, later *foxg1* expression and a larger pallium. Manipulation of the Hedgehog and Wingless pathways in cichlid and zebrafish embryos is sufficient to mimic differences between rock- versus sand-dweller brains. Our data suggest that competing ventral Hedgehog and dorsal Wingless signals mediate evolutionary diversification of the telencephalon.

¹Parker H. Petit Institute for Bioengineering and Biosciences, School of Biology, Georgia Institute of Technology, Atlanta, Georgia 30332, USA. ²Department of Physiology, Development and Neuroscience, University of Cambridge, Downing Street, Cambridge CB2 3DY, UK. ³Medical Research Council Centre for Developmental Neurobiology, King's College London, London SE1 1UL, UK. Correspondence and requests for materials should be addressed to J.T.S. (email: todd.strelman@biology.gatech.edu)

Adult derivatives of the telencephalon are singularly important in evolution and neurological disease. The dorsal-most component (the cerebral cortex) is acutely enlarged in mammals¹, and this expansion may have prefigured new forms of communication, reasoning and memory in human ancestors². The ventral portion, collectively called basal ganglia, controls complex motion and emotion. All jawed vertebrates possess a telencephalon and share an embryological division into dorsal (the pallium) and ventral (subpallium) territories³. The parts of the telencephalon (that is, cortex and ganglia) integrate brain function via networks of excitatory and inhibitory neurons that originate from the pallium and subpallium, respectively^{4–7}. Notably, a balance between pallium-derived excitatory neurons and inhibitory neurons from the subpallium is necessary for proper social and sensory function. In fact, misbalance between these neuronal types may be a common facet of heterogeneous syndromes like autism and schizophrenia^{8,9}.

Studies in model organisms elucidate how cellular and molecular processes construct the telencephalon and its dorsal/ventral (DV) derivatives⁶. The telencephalon develops under the influence of ventral Hedgehog (Hh) and dorsal Wingless (Wnt) signals^{10,11}. These morphogens are part of distinct, interacting pathways that pattern the entire neural tube¹². In the zebrafish, the transcription factor *foxl1* mediates DV cross-talk between Hh and Wnt signals¹³. Specifically, *shh* induces the expression of *foxl1* in the presumptive telencephalon at neurula stage. *foxl1* is required for ventral telencephalic fate^{14,15} and directly inhibits the dorsalizing effects of *wnt8b* in the dorsal midline¹³. Despite the importance of DV telencephalon specification in evolution and disease⁷, the mechanisms generating natural diversity in pallium and subpallium proportions are largely unknown.

The evolutionary developmental pathways that shape regions of the telencephalon can be explored using cichlid fishes from Lake Malawi (East Africa). Despite large variation in brains and

behaviours^{16,17}, genomic differences among lineages, species and populations are small^{18,19}. Malawi rock dwellers (locally and hereafter called ‘mbuna’) are strongly territorial and aggressive; they breed and feed at high density in complex three-dimensional habitats. Most mbuna eat algae from the substratum. Adult mbuna brains exhibit enlarged anterior components: telencephalon and olfactory bulbs^{16,17}. Sand dwellers (locally called ‘utaka’, hereafter called non-mbuna) are less site-specific and less aggressive. They breed on seasonal leks where males build sand bowers to attract females. Many non-mbuna capture small prey using acute vision. Their brains are elaborated for more caudal structures: optic tecta, thalamus and eyes^{16,17}.

We show that partitioning of the telencephalon into pallial and subpallial domains differs in mbuna versus non-mbuna cichlids because of integrated divergence in Hh and Wnt signals, along DV and anterior–posterior (AP) developmental neuraxes. The differences that we observe between these two Malawi ecotypes are heterochronic and quantitative. Therefore, we experimentally antagonize and enhance Hh/Wnt signalling using small

Table 1 | Manipulation of Hh and Wnt signals changes cichlid and zebrafish pallial/subpallial compartments.

| a | % Pal | % SPal |
|---|------------|------------|
| Mbuna (N = 16) | 39.0 ± 4.0 | 61.0 ± 4.0 |
| Mbuna _{DMSO} (N = 13) | 38.7 ± 3.9 | 61.3 ± * |
| Mbuna _{Cyclo} (N = 17) | 58.4 ± 3.4 | 41.6 ± * |
| Mbuna _{LiCl} (N = 14) | 57.6 ± 2.7 | 42.4 ± * |
| NMbuna (N = 16) | 58.3 ± 2.1 | 41.7 ± * |
| NMbuna _{DMSO} (N = 8) | 56.3 ± 1.8 | 43.7 ± * |
| NMbuna _{SAG} (N = 11) | 40.6 ± 5.0 | 59.4 ± * |
| NMbuna _{IWR} (N = 9) | 38.4 ± 5.9 | 61.6 ± * |
| b | | |
| <i>D.r.</i> _{Cyclo} (N = 11) | 61.2 ± 3.2 | 38.8 ± * |
| <i>D.r.</i> _{LiCl} (N = 5) | 62.7 ± 2.7 | 37.3 ± * |
| <i>D.r.</i> _{BIO} (N = 7) | 63.4 ± 3.9 | 36.6 ± * |
| <i>D.r.</i> _{DMSO} (N = 6) | 55.5 ± 2.3 | 44.5 ± * |
| <i>D.r.</i> (N = 10) | 55.2 ± 1.8 | 44.8 ± * |
| <i>D.r.</i> _{HS control} (N = 7) | 55.2 ± 2.0 | 44.8 ± * |
| <i>D.r.</i> _{dnTcf3HS} (N = 8) | 46.2 ± 4.7 | 53.8 ± * |
| <i>D.r.</i> _{shh inj.} (N = 17) | 34.0 ± 6.0 | 66.0 ± * |

BIO, 6-bromoindirubin-3'-oxime; DMSO, dimethylsulphoxide; *D.r.*, *Danio rerio*; HS, heat shock; Pal, pallial; SPal, subpallial.

We show the volumetric percentage of the total telencephalon occupied by the % Pal and % SPal. Pal and Spal percentages represent components of the same whole, thus the s.d. is the same for both, indicated by the asterisk '*'. (a) Values represent the mean from several individuals of three mbuna (6 *Cynotilapia afra* (CA), 5 *Labeotropheus fuelleborni* (LF) and 5 *Maylandia zebra*) and three non-mbuna species (6 *Aulonocara jacobfreibergi* (AJ), 4 *Copadichromis borleyi* (CB) and 6 *Mchenga conophoros* (MC)), ± 1 s.d. In addition, we show percentages for small-molecule-treated morphants (cyclopamine, LiCl, SAG and IWR) and vehicle controls (DMSO). Species × treatment N = cyclopamine 6 CA, 5 LF, 6 *Maylandia zebra* (MZ); LiCl 5 CA, 5 LF, 4 MZ; SAG 4 AJ, 2 CB, 5 MC; IWR 2 AJ, 3 CB, 4 MC. (b) Values represent the mean of several *D.r.* individuals, ± 1 s.d. Data are arranged into treatment groups that are (i) similar to non-mbuna (for example, BIO, LiCl and cyclopamine), (ii) WT plus controls and (iii) similar to mbuna (dnTcf3HS, *shh* injection).

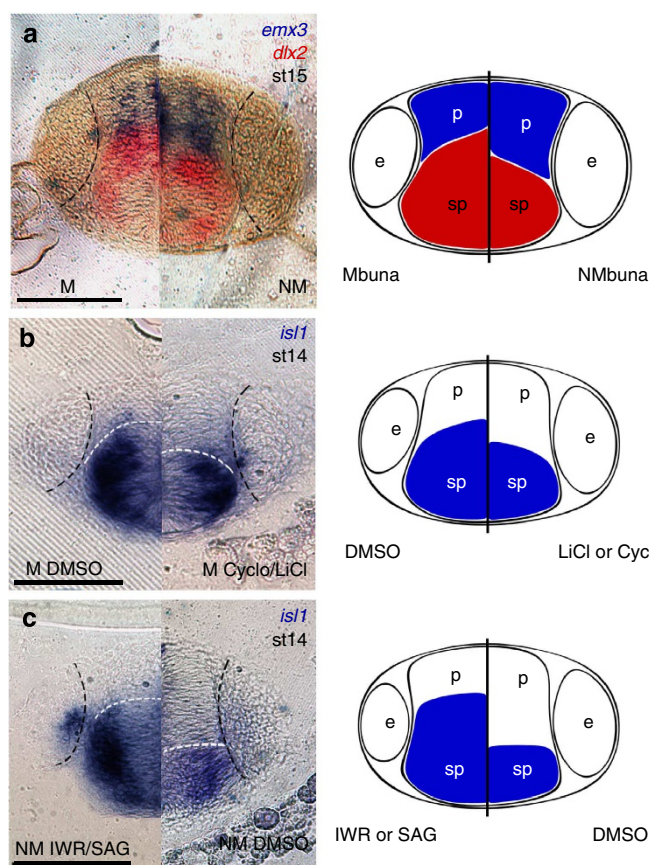


Figure 1 | Cichlid rock versus sand dwellers differ in pallial/subpallial proportions. (a–c) Left panels are transverse sections of the telencephalon at its greatest DV extent, and right panels are schematics of data depicted on the left. Black-dotted lines represent the position and size of the eyes in each section; note variance in eye size. Scale bar, 100 µm. (a) A ‘split-screen’ double ISH of *emx3* (blue) and *dlx2* (red) used to visualize the pallium and subpallium in mbuna, left, and non-mbuna, right. (b) Expression of the subpallial marker *is11* is depicted, and an expansion of the pallium (above dotted white line) in cyclopamine- or LiCl-treated mbuna (right side) versus DMSO control mbuna (left) is shown. (c) An expansion of the subpallium (below dotted white line) in SAG- or IWR-treated non-mbuna (left side) versus DMSO control non-mbuna (right) is shown. The treated specimens in summary panels **b** and **c** are cyclopamine-treated mbuna and IWR-treated non-mbuna, respectively.

molecules, in multiple species of mbuna versus non-mbuna and the zebrafish, to mimic natural diversity. Our data demonstrate how variation in early development works to specify evolutionary diversification of forebrain structures.

Results

Telencephalon DV organization of mbuna and non-mbuna differs. After the pallial–subpallial boundary (PSB) is established during stage 13 (late somitogenesis)²⁰, and before telencephalon eversion (late pharyngula, stage 16), the pallium and subpallium can be visualized and measured *in toto*, in transverse section. Mbuna embryos possess proportionally larger subpallial, and non-mbuna exhibit the opposite, larger pallia (Student's *t*-test, $n = 16$ for each of mbuna and non-mbuna, $t = 17.218$, $P < 0.001$, Fig. 1a; Table 1a shows data for three diverse species of mbuna and non-mbuna each, measured at stages 14 and 15). This can be nicely observed at stage 15 (equivalent to zebrafish prim-18), where the pallium is marked by *emx3* expression and the subpallium by *dlx2*. Figure 1a shows a transverse section through the telencephalon and uses a split-screen effect to demonstrate proportional differences between mbuna (left half-image) and non-mbuna (right half-image), assuming symmetry.

Telencephalon divergence is mediated by Hh and Wnt signals. We aimed to understand how evolutionary differences in the

mbuna versus non-mbuna telencephalon are established. As cichlid embryos exit neurula stage, mbuna *shh* shows a larger DV domain, relative to non-mbuna, in its anterior-most area of expression (Fig. 2a versus Fig. 2d). By 4–5 somites, stronger *shh* activity in mbuna is correlated with *foxg1* expression in the presumptive telencephalon (Fig. 2e,i). The non-mbuna *shh* domain is more ventrally restricted, expands dorsally more slowly and subsequent *foxg1* in non-mbuna is delayed (Fig. 2h,l). Non-mbuna *foxg1* is not expressed in the presumptive telencephalon until mid-stage 11 (8–10 somites).

Although mbuna elaborate Hh signalling along the DV axis, non-mbnas are characterized by increased Wnt activity along the AP axis. Like *wnt1*, *wnt8b* progresses more rapidly from the midbrain–hindbrain boundary into the presumptive midbrain and diencephalon¹⁷. *wnt8b* enters the telencephalon at stage 11, following initial development of the pre-zona limitans intrathalamica¹⁷ (pre-ZLI; Fig. 3). In non-mbuna, *wnt8b* is expressed in the telencephalon slightly before, or upon induction of *foxg1* (7 somites); in mbuna, *foxg1* has been expressed for approximately 10 h before *wnt8b*. Differences in the size of the *foxg1* domain are apparent at this stage (Fig. 2m,p). The pallium and subpallium are then demarcated by the PSB at stage 13 (Fig. 1).

Because of spatial and temporal differences in expression of Hh and Wnt ligands in cichlid telencephalon patterning¹⁷ (Fig. 2), we examined the activity of receptors and effectors in these pathways

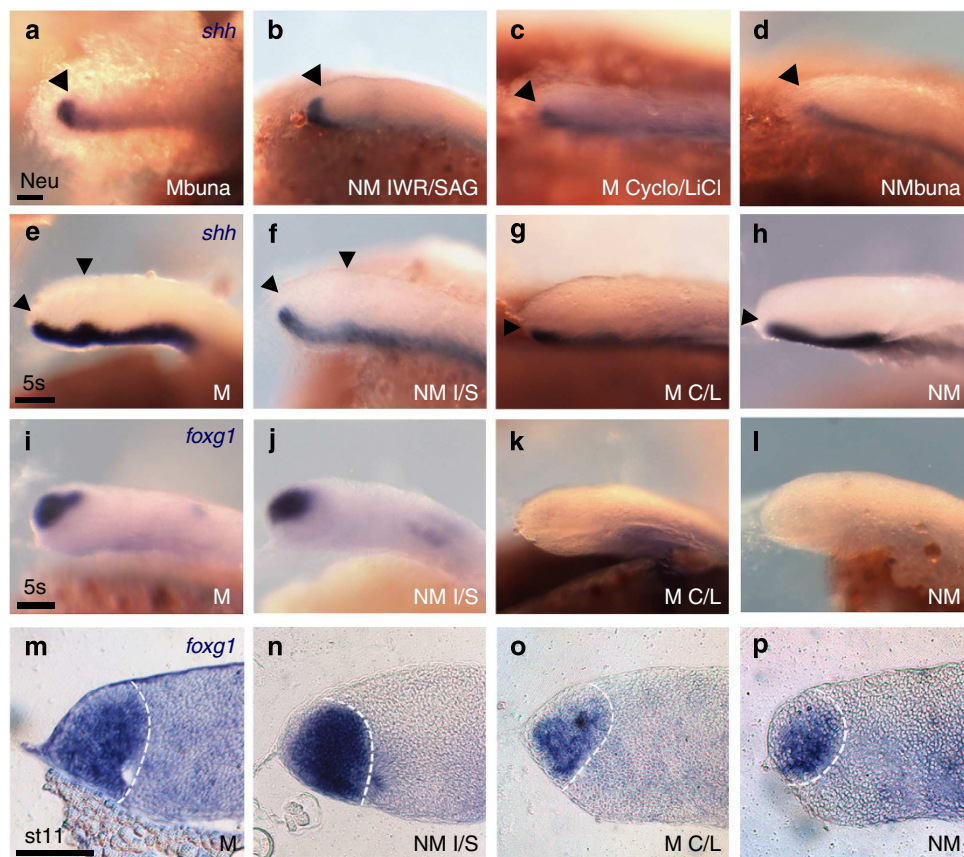


Figure 2 | Natural and experimental variation in the Hh and Wnt pathways modulates the pallial/subpallial gene circuit. (a–l) Images are lateral images of whole-mount embryos, anterior to the left. Neu in a–d and 5s in e–l refer to neurula and five somite stages, respectively. Panels m–p are midline, sagittal sections of embryos during late stage 11 (st11, 10–12 s). All panels from left to right are untreated mbuna (M), IWR- or SAG-treated non-mbuna (I/S), cyclopamine- or LiCl-treated mbuna (C/L) and untreated non-mbuna (NM). Specific treatments shown in the two summary (middle) columns are: b—IWR-treated (1 μ M) NMBuna, c—cyclopamine-treated (50 μ M) Mbuna, f—SAG-treated (1 μ M) NM, g—LiCl-treated (1.25 M) M, j—SAG NM, k—cyclopamine M, n—IWR NM and o—LiCl M. Scale bar, 50 μ m (applied to all four panels per row). (a–h) Arrowheads point to the dorsal progression of *shh* expression. (m–p) Dotted white lines outline the presumptive telencephalon.

(Fig. 4). As expected, in neurula and at 5 somites, *ptc1* (a receptor for *shh*) is expressed in the majority of the neural tube in mbuna, but is confined to a small ventral portion in non-mbuna (Fig. 4b,d). In model organisms, Gli3 integrates Hh and Wnt function. It is unclear what factors induce Gli3 in the forebrain¹⁰, but it is cleaved into a Hh-repressor form (Gli3R) where Hh activity is low²¹. Gli3R is a positive regulator of Wnt signalling in the forebrain^{22,23}, and Wnt activates Gli3R specifically, via β -catenin^{24–26}. Gli3R is necessary for proper specification of the pallium and this likely involves mutual repression of Hh¹¹, and/or perhaps *Foxg1*¹³. In cichlids, *gli3* is pan-expressed in the anterior forebrain at neurula (Fig. 4a) but begins to recede dorsally in the presumptive telencephalon. In mbuna, *foxg1* is induced, presumably by *shh*, at 4–5 somites (Fig. 2) and is co-expressed with *gli3* (Fig. 4c) for ~12 h (until stage 12, mid-somitogenesis). In non-mbuna, *foxg1* is induced later (Fig. 2) and *gli3* expression takes longer to recede (the two are co-expressed until stage 13). Intriguingly, β -catenin, an effector of the canonical Wnt pathway, is upregulated 4–5 h before *wnt8b* expression in the telencephalon, and this upregulation occurs earlier in non-mbuna cichlids (Fig. 4e). Note that β -catenin expression is grossly similar between mbuna and non-mbuna in more posterior serial sections from the same embryos (Fig. 4e, grey arrow and inset images).

Manipulation of Hh and Wnt signals mimics mbuna versus non-mbuna. Our comparative data suggest that mbuna versus non-mbuna pallial/subpallial proportions differ due to quantitative changes in Hh and Wnt signalling. To test this hypothesis, we used small-molecule activators and antagonists to manipulate the Hh and Wnt pathways in both mbuna and non-mbuna embryos. Treatment of mbuna embryos with 50 μ M cyclopamine, a Hh antagonist, for a brief window during neurula, knocks down *shh*

expression and slows its progression dorsally during somitogenesis (Fig. 2c,g); this treatment phenocopies *shh* expression in non-mbuna. Conversely, treatment of non-mbuna embryos with the Hh agonist smoothed agonist (SAG) (1 μ M) during neurula causes an expansion of *shh* expression in early somitogenesis, mimicking mbuna embryos (Fig. 2b,f). Notably, treatment of mbuna embryos with the Wnt activator lithium chloride (LiCl) (1.25 mM) phenocopies both the cyclopamine mbuna morphants and non-mbuna embryos, whereas treatment of non-mbuna with the Wnt antagonist inhibitor of Wnt response 1 (IWR-1) (1 μ M) phenocopies the SAG non-mbuna morphants and mbuna embryos (Fig. 2b,c,f,g).

Upregulation of Hh (SAG treatment) and downregulation of Wnt (IWR treatment) are sufficient to induce *foxg1* earlier in non-mbuna morphants, whereas downregulation of Hh (cyclopamine) and upregulation of Wnt (LiCl) in mbuna morphants reproduce the delayed expression of *foxg1* observed in non-mbuna embryos (Fig. 2j,k). Treatments at neurula stage similarly phenocopy differences in size of the *foxg1* expression domain between mbuna and non-mbuna at stage 11 (Fig. 2n,o). Finally, we investigated the effect of treatment (again at neurula) on

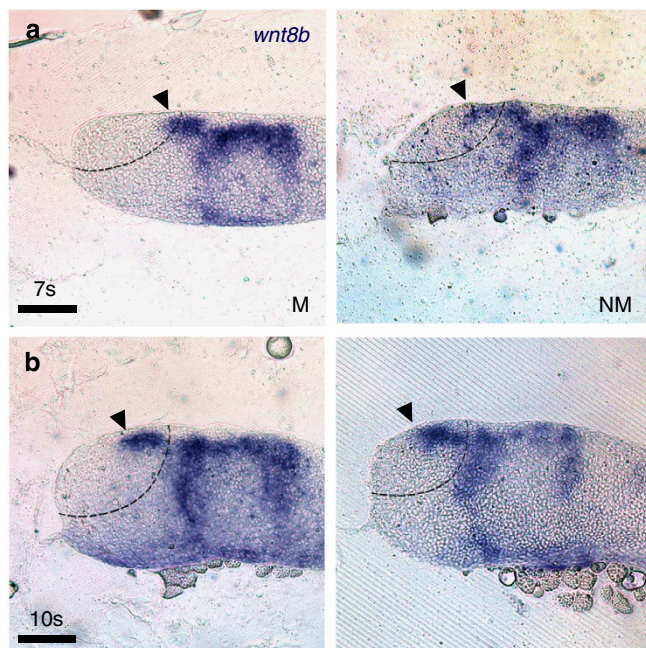


Figure 3 | *wnt8b* is first expressed in the cichlid telencephalon during mid-stage 11. For all panels, mbunas (Ms) are on the left, and non-mbunas (NMs) are on the right. Images are sagittal, midline sections. Scale bar, 50 μ m. (a) *wnt8b* expression is shown as it enters the telencephalon at 7 somites (7s). Arrows note the greater AP progression of *wnt8b* expression in NM versus M. (b) *wnt8b* reaches its greatest AP extent in the telencephalon at 10s.

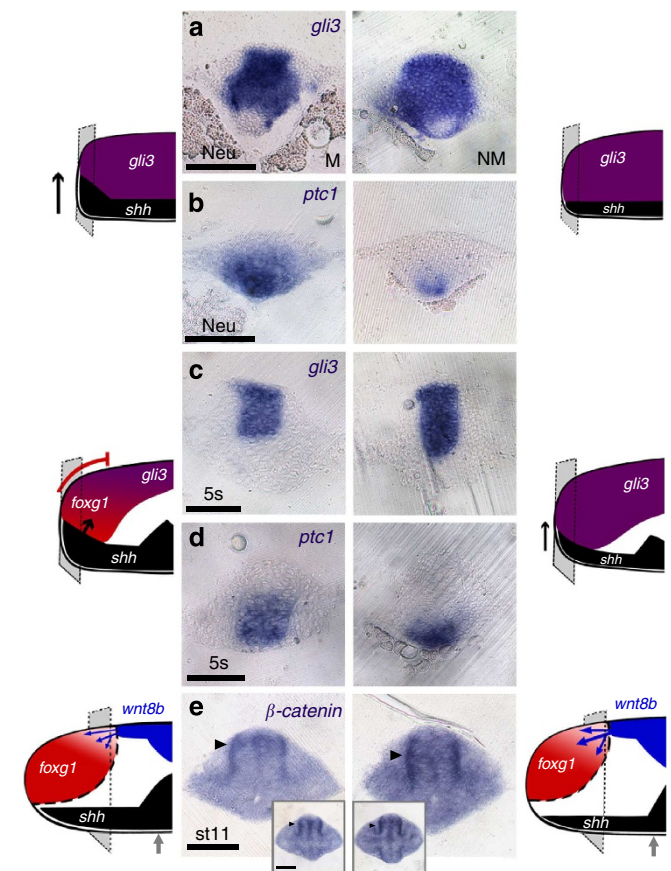


Figure 4 | Activity of the Hh and Wnt pathways during cichlid DV telencephalon patterning. Images are transverse sections of cichlid embryos. Scale bar, 50 μ m. For all panels, mbunas (Ms) are on the left and non-mbunas (NMs) are on the right. At far left and right, schematics review the action of genes in the pallial/subpallial circuit (see Fig. 2) and show the position of the transverse sections (dotted grey rectangles). (a–d) Expression of *gli3*, a mediator of Hh/Wnt signalling, and *ptc1*, a receptor for *shh*, at neurula and 5 somites. (e) Activity of β -catenin in the forebrain during stage 11 (st11). Black arrowheads point to the DV signal of β -catenin in the diencephalon; grey arrows in the schematics show the AP position of the inset panels.

pallial/subpallial proportions 48 h later, during stages 14 and 15. Manipulation of either Hh (cyclopamine-treated, $n = 17$, versus dimethylsulphoxide (DMSO) controls, $n = 13$, $t = 14.468$, $P < 0.001$; SAG, $n = 11$, versus DMSO, $n = 8$, $t = 9.574$, $P < 0.001$) or Wnt (LiCl, $n = 14$, versus DMSO, $n = 13$, $t = 14.540$, $P < 0.001$; IWR, $n = 9$, versus DMSO, $n = 8$, $t = 8.629$, $P < 0.001$) pathways is sufficient to change pallial/subpallial organization from mbuna to non-mbuna proportions, and *vice versa* (Fig. 1b,c; Table 1a shows percentages for multiple neurula-treated mbuna and non-mbuna species).

By varying the timing of manipulation with small molecules, we illustrate a narrow window of sensitivity for cross-talk between ventral and dorsal signals. Treatment of mbuna with cyclopamine after neurula (for example, during early somitogenesis) does not alter the onset of *foxg1* expression, nor does it result in a larger pallium. Similar temporal specificity applies to non-mbuna; SAG treatment during somitogenesis does not induce earlier *foxg1* expression, nor does it expand the subpallium. Conversely, upregulation of Wnt (LiCl) in mbuna phenocopies non-mbuna as long as treatment occurs before the induction of *foxg1* at 4–5 somites. However, the effect of Wnt antagonism (IWR) in non-mbuna diminishes if treatment occurs after neurula stage. This time line implicates a factor that (i) limits the efficacy of Hh manipulation after neurula stage, (ii) responds flexibly to Wnt signals, (iii) but can act independently of them. We suggest that mbuna and SAG/IWR-treated non-mbuna possess a telencephalon that has been ventralized by Hh signal acting through early *foxg1* expression to counteract dorsalizing factors. In contrast, non-mbuna and cyclopamine/LiCl-treated mbuna possess a telencephalon that has been dorsalized by *gli3*/Wnt activity that precedes *foxg1* expression.

To explore the generality of our treatment results, we manipulated pallial/subpallial proportions in the zebrafish. We first quantified pallial and subpallial volumes in wild-type (WT) zebrafish prim-18 stage (equivalent to stage 15 cichlids). The pallial percentage for zebrafish is comparable to values observed in non-mbuna (Table 1b). As in cichlids, an increase in Wnt signal (Student's *t*-test, 0.2 M LiCl, $n = 5$, versus DMSO controls, $n = 6$, $t = 4.819$, $P < 0.001$; 4 μ M 6-bromoindirubin-3'-oxime, $n = 7$, versus DMSO, $n = 6$, $t = 4.367$, $P < 0.001$) or a decrease in Hh activity (pooled 12 and 24 μ M cyclopamine-treated, $n = 11$, versus DMSO, $n = 6$, $t = 3.860$, $P < 0.001$) is sufficient to expand the pallium at the expense of subpallium (Table 1b). In addition, zebrafish embryos were injected with *shh* mRNA at the 1–2 cell stage to increase Hh. Measurements at prim-18 show an expansion of the subpallium, similar to proportions observed in mbuna and SAG-treated non-mbuna cichlids (pooled 20, 40 and 80 pg of injected *shh* zebrafish morphants, $n = 17$, versus WT controls, $n = 10$, $t = 10.824$, $P < 0.001$, Table 1b; Fig. 5). Finally, down-regulation of the Wnt pathway via a dominant-negative *tcf3* HS-activated construct¹³ similarly results in a telencephalon with expanded subpallium (dnTcf3HS morphants, $n = 8$, versus HS controls, $n = 7$, $t = 4.68$, $P < 0.001$, Table 1b; Fig. 5). Taken together, our manipulative experiments suggest that ventral Hh and dorsal Wnt signals interact to pattern the pallium and subpallium across bony fishes, despite differences in the timing of pathway activity between cichlids and zebrafish.

Discussion

Cichlid and zebrafish brains develop at different rates, and this comparison is informative for models of telencephalon patterning. For instance, in the zebrafish, *shh* reaches the ventral presumptive telencephalon (anterior medial neural plate) first, immediately followed by *foxg1*; *wnt8b* appears in the telencephalic roof by 5–6 somites¹³. Cichlids show a greater time lag in

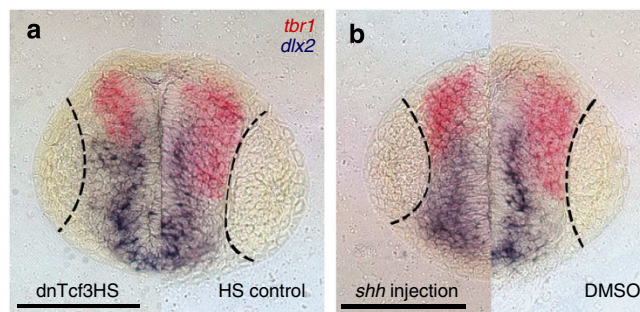


Figure 5 | Manipulation of Hh and Wnt signalling affects pallial/subpallial proportions in the zebrafish. Panels are frontal sections of *D. rerio* embryos, showing the telencephalon at its greatest DV extent. Embryos are collected 32 h post fertilization or prim-18. Black-dotted lines represent the position and size of the eyes in each section; note variance in eye size. Scale bar, 100 μ m. Both **a** and **b** are split-screen double ISH of *tbr1* (red) and *dlx2* (blue), used to visualize the pallium and subpallium, respectively. **(a)** The effect of HS-activated dominant-negative *tcf3* (dnTcf3HS) is shown, an effector of the Wnt pathway (left side), compared with HS controls (right). **(b)** Split screen of an embryo injected at the one- to two-cell stage with 20 pg *shh* mRNA (left side) compared with a WT control (WT, right). These treatments (\downarrow Wnt, \uparrow Hh) mimic mbuna cichlids (see Fig. 1).

the appearance of these molecules and dual heterochronic variation between mbuna and non-mbuna, along both DV and AP neuraxes (Fig. 6a). A simple model to explain telencephalon divergence between mbuna and non-mbuna begins with the initial difference in *shh* expression at neurula and the concomitant heterochrony in *foxg1* expression (Fig. 6a,b). Note that the cichlid *wnt8b* promoter possesses vertebrate-conserved binding sites for *foxg1* (ref. 13). The lag in timing between cichlid *shh* and *foxg1* expression suggests that Hh signals may not induce *foxg1* directly, and/or that a threshold of Hh/Gli complex activity is required for induction¹³.

Because Wnt ligands do not enter the cichlid telencephalon until stage 11, our observations from comparative expression and small-molecule treatments (at neurula) require an early acting, anti-Hh factor, sensitive to induction by Wnt/ β -catenin. We suggest that *gli3* serves this role and that, in particular, Gli3R acts first (before 7–8 somites) as an early dorsalizing factor and then later as a dorsal analogue of ventral *foxg1*, integrating Hh and Wnt signals to pattern telencephalic diversity (Fig. 6).

Overall, Hh and Wnt morphogens compete for influence along the DV axis of the entire brain, throughout ontogeny^{11,12,27}. For example, it has been shown that eye loss and elaboration of the ventral forebrain in cavefish is partly explained by expansion of midline *shh* expression^{28,29}. We demonstrate here how natural variation in telencephalon patterning evolves via temporal, spatial and quantitative tuning of both the Hh and Wnt pathways along integrated DV and AP neuraxes. Notably, our data combined with an earlier report¹⁷, suggest that, at least in Malawi cichlids, a large subpallium is the by-product of a large telencephalon, precisely because the evolutionary differences that we identify commence early in development. In the six mbuna and non-mbuna species that we studied, each have unique adult brains^{16,17}, but exhibit little heterogeneity within groups at patterning stages. This implies an early neural blueprint for rock versus sand dwellers that is later elaborated for species-specific lifestyles and ecologies. Embryonic differences in the size of telencephalic compartments may thus facilitate, and also constrain variation in neuronal specification, sensory performance and social biology^{30,31}.

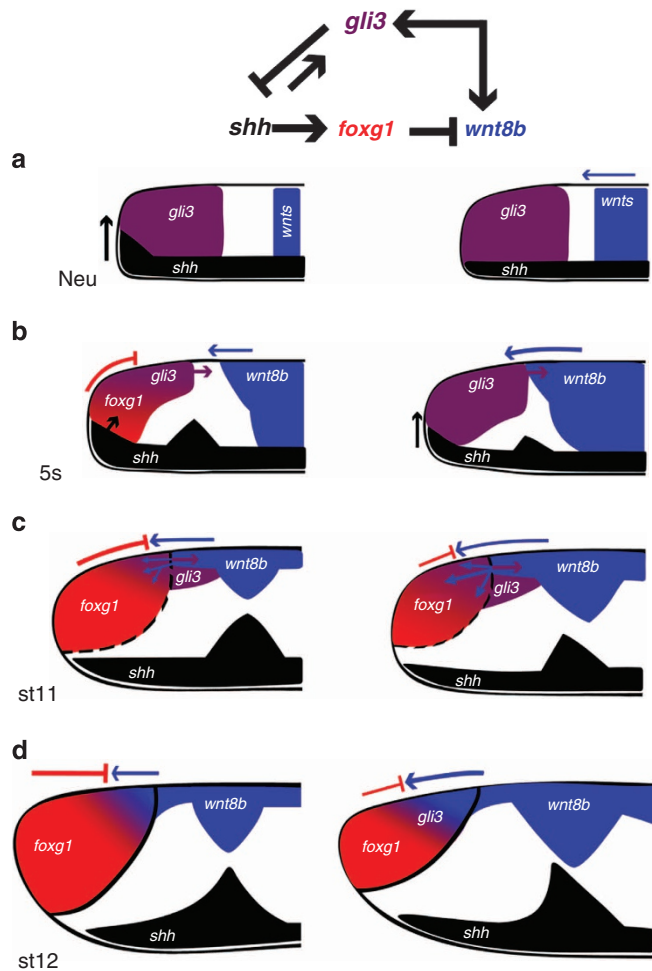


Figure 6 | Competing Hh and Wnt signals drive divergent pallial/subpallial patterning. At top, we illustrate the gene network that establishes pallial/subpallial proportions (see also Ulloa and Marti¹²). Arrows indicate positive signal; T bars indicate negative interactions. For all panels, mbunas are on the left, and non-mbunas are on the right. All schematics are lateral, midline representations. Neu, neurula; 5s, 5 somites; st11, stage 11 (6–12 somites); st12, stage 12 (13–20 somites). (a) Greater DV progression of *shh* expression in mbuna versus greater AP deployment of Wnt in non-mbuna. (b) Increased *shh* in mbuna leads to earlier induction of *foxg1*, by 4–5s. *gli3* is present in the presumptive telencephalon of mbuna and non-mbuna, counteracted by *foxg1* in mbuna only. (c) As *wnt8b* enters the telencephalon, mbuna *foxg1* has been established for some time. Non-mbuna *foxg1* is first expressed in the telencephalon slightly after *wnt8b*. (d) Early elaboration of *foxg1* in mbuna and *gli3/wnt8b* in non-mbuna establishes contrasting readouts of ventralizing versus dorsalizing signals, at stage 12.

Methods

Telencephalon measurements. Volumes of pallial and subpallial compartments were measured by integrating over transverse sections of the telencephalon in staged embryos of mbuna and non-mbuna species. Mbuna species included *Cynotilapia afra* (planktivore), *Labeotropheus fuelleborni* (algivore) and *Maylandia zebra* (generalist); non-mbuna species included *Aulonocara jacobfreibergi* ('sonar' hunter), *Copadichromis borleyi* (planktivore) and *Mchenga conophoros* (insectivore/generalist). We measured embryos at stages 14 and 15, following the first point (stage 13)^{17,20} at which the pallium and subpallium can be distinguished by cellular boundaries (for example, the PSB). Proportions are consistent across stages 13–15, until telencephalon eversion (stage 16). We used gene expression to help visualize the PSB and telencephalic compartments: the pallium can be marked by *pax6*, *emx3* or *tbr1* expression, and the subpallium by *dlx2* or *isl1* (see below for *in situ* hybridization (ISH)).

Measurements were made using ImageJ on scaled images of transverse sections. We used morphological landmarks (for example, the anterior commissure ventrally

and the epithalamus dorsally) to maintain consistency across individuals and species. Between 10 and 20 individuals (from multiple broods), per species were sectioned and prepared for measurement. To simplify analysis, individuals with oblique sections were eliminated, leaving 4–6 individuals per species. Pallial and subpallial measurements were expressed as a percentage of the total telencephalon. As the telencephalon encompasses more than one sequential transverse section, we used the Cavalieri method³² (Σ (area of each section) * (distance between sections)) to express volumetric percentages.

In situ hybridization. ISH experiments are based on previously published protocols for cichlids³³. Probes were constructed from cDNA sequences derived from partial genome assemblies of Lake Malawi cichlids¹⁹. The RNA probes are identical across the cichlid species used in this study. All ISH experiments were performed with multiple specimens (multiple individuals within single broods, then repeated at least twice with alternative broods) to fully characterize expression patterns within and across species. Once ISH was complete, embryos were embedded in gelatin-albumin blocks and sectioned¹⁷.

Manipulation with small molecules. Embryos from three mbuna species *L. fuelleborni*, *M. zebra* and *C. afra* were treated with LiCl, an activator of the Wnt pathway, or cyclopamine, an antagonist of the Hh pathway. The LiCl 1 M stock solution and 1.25 mM working concentration were prepared as described in Sylvestre *et al.*¹⁷ A 5 mM cyclopamine stock was used to obtain the final working concentration of 50 μ M. Complementary experiments were performed using non-mbuna species *A. jacobfreibergi*, *C. borleyi* and *M. conophoros*. Embryos were treated with a Hh agonist, SAG (Enzo Life Sciences)³⁴, or a Wnt antagonist, IWR-1 (Enzo Life Sciences)³⁵. Stock and working concentrations for both SAG and IWR are 100 and 1 μ M, respectively.

Embryos in broods (one brood consists of 20–40 individuals) from each species of mbuna and non-mbuna were treated during neurula stage (approximately 36–40 h post fertilization) for 5 h at 28 °C, and bathed with either a chemical or DMSO vehicle controls (0.125% for LiCl; 1% for cyclopamine, SAG and IWR). Experiments were repeated with 2–4 additional broods for each species. After treatment, embryos were washed twice with fish water, placed in culture flasks with fresh fish water and incubated at 28 °C until they reached the desired stage. Treatment and control embryos were post-processed (ISH, sectioning and measurements) identically to descriptions above for untreated embryos. Additional experiments were conducted into early somitogenesis to identify the temporal window of sensitivity to treatment.

Danio rerio experiments and processing. WT zebrafish embryos were cultured in embryo media E2, then treated from bud to five somite stage with 1% DMSO and one of the following chemicals: 0.2 M LiCl (BDH Chemicals) or 4 μ M 6-bromoindirubin-3'-oxime (Sigma-Aldrich) to promote Wnt/ β -catenin signalling; or 12/24 μ M cyclopamine (Sigma-Aldrich) to inactivate Hh. Embryos were washed twice with E2 and then incubated until prim-18 (32 h.p.f. at 28.5 °C). They were then fixed in 4% paraformaldehyde for 4 h at room temperature or overnight at 4 °C and afterwards washed with PBS and stored in methanol at –20 °C.

In addition to treatment with small molecules, gene levels were manipulated directly. To downregulate Wnt signal, transgenic (Hsp70: Δ Tcf3-GFP)¹³ embryos were heat shocked at the tailbud stage for 30 min at 37 °C, incubated at 28 °C and fixed at prim-18. To upregulate Hh signal, *shh* mRNA for microinjection was prepared by digesting pSP64T-*shh* with *Bam*HI and transcribing with Sp6 polymerase (Ambion). The RNA was subsequently purified using the RNeasy kit (Qiagen), and 20, 40 or 80 pg was injected into one- to two-cell stage embryos. Embryos were cultured until prim-18 and fixed in paraformaldehyde as above. Embryos were then stained for *dlx2* and *tbr1* expression via double ISH to visualize and measure pallial–subpallial proportions as described for cichlid embryos (see above).

References

- Rowe, T. B., Macrini, T. E. & Luo, Z. X. Fossil evidence on origin of the mammalian brain. *Science* **332**, 955–957 (2011).
- Butler, A. B. & Hodos, W. *Comparative Vertebrate Neuroanatomy: Evolution and Adaptation* 2nd edn (John Wiley & Sons Inc., Hoboken, NJ, 2005).
- Moreno, N., González, A. & Rétaux, S. Development and evolution of the subpallium. *Semin. Cell Dev. Biol.* **20**, 735–743 (2009).
- Cobos, I., Puelles, L. & Martínez, S. The avian telencephalic subpallium originates inhibitory neurons that invade tangentially the pallium (dorsal ventricular ridge and cortical areas). *Dev. Biol.* **239**, 30–45 (2001).
- Cocas, L. A. *et al.* *Pax6* is required at the telencephalic pallial–subpallial boundary for the generation of neuronal diversity in the postnatal limbic system. *J. Neurosci.* **31**, 5313–5324 (2011).
- Hébert, J. M. & Fishell, G. The genetics of early telencephalon patterning: some assembly required. *Nat. Rev. Neurosci.* **9**, 678–685 (2008).
- Hansen, D. V., Rubenstein, J. L. R. & Kriegstein, A. R. Deriving excitatory neurons of the neocortex from pluripotent stem cells. *Neuron* **70**, 645–660 (2011).

8. Rubenstein, J. L. R. & Merzenich, M. M. Model of autism: increased ratio of excitation/inhibition in key neural systems. *Genes Brain Behavior* **2**, 255–267 (2003).
9. Yizhar, O. *et al.* Neocortical excitation/inhibition balance in information processing and social dysfunction. *Nature* **477**, 171–178 (2011).
10. Altaba, A. R., Palma, V. & Dahmane, N. Hedgehog-Gli signalling and the growth of the brain. *Nat. Rev. Neurosci.* **3**, 24–33 (2002).
11. Rallu, M., Corbin, J. G. & Fishell, G. Parsing the prosencephalon. *Nat. Rev. Neurosci.* **3**, 943–951 (2002).
12. Ulloa, F. & Marti, E. Wnt won the war: antagonistic role of Wnt over Shh controls dorso-ventral patterning of the vertebrate neural tube. *Dev. Dyn.* **239**, 69–76 (2010).
13. Danesin, C. *et al.* Integration of telencephalic Wnt and Hedgehog signaling center activities by Foxg1. *Dev. Cell* **16**, 576–587 (2009).
14. Roth, M. *et al.* Foxg1 and TLE2 act cooperatively to regulate ventral telencephalon formation. *Development* **137**, 1553–1562 (2010).
15. Manuel, M. *et al.* The transcription factor foxg1 regulates the competence of telencephalic cells to adopt subpallial fates in mice. *Development* **137**, 487–497 (2010).
16. Huber, R., van Staaden, M. J., Kaufman, L. S. & Liem, K. F. Microhabitat use, trophic patterns, and the evolution of brain structure in African cichlids. *Brain Behavior Evol.* **50**, 167–182 (1997).
17. Sylvester, J. B. *et al.* Brain diversity evolves via differences in patterning. *Proc. Natl Acad. Sci. USA* **107**, 9718–9723 (2010).
18. Meyer, A., Kocher, T. D., Basasibwaki, P. & Wilson, A. C. Monophyletic origin of Lake Victoria cichlid fishes suggested by mitochondrial DNA sequences. *Nature* **347**, 550–553 (1990).
19. Loh, Y.-H. E. *et al.* Comparative analysis reveals signatures of differentiation amid genomic polymorphism in lake malawi cichlids. *Genome Biol.* **9**, R113 (2008).
20. Fujimura, K. & Okada, N. Development of the embryo, larva and early juvenile of Nile tilapia *Oreochromis niloticus* (pisces: cichlidae): developmental staging system. *Dev. Growth Differ.* **49**, 301–324 (2007).
21. Blaess, S., Corrales, J. D. & Joyner, A. L. Sonic hedgehog regulates Gli activator and repressor functions with spatial and temporal precision in the mid/hindbrain region. *Development* **133**, 1799–1809 (2006).
22. Mullor, J. L., Dahman, N., Sun, T. & Altaba, R. A. Wnt signals are targets and mediators of Gli function. *Curr. Biol.* **11**, 769–773 (2001).
23. Fotaki, V., Price, D. J. & Mason, J. O. Wnt/ β -catenin signaling is disrupted in the extra-toes (Gli3(Xt/Xt)) mutant from early stages of forebrain development, concomitant with anterior neural plate patterning defects. *J. Comp. Neurol.* **519**, 1640–1657 (2011).
24. Alvarez-Medina, R., Le Dreau, G., Ros, M. & Marti, E. Hedgehog activation is required upstream of Wnt signalling to control neural progenitor proliferation. *Development* **136**, 3301–3309 (2009).
25. Li, X. J. *et al.* Coordination of sonic hedgehog and Wnt signaling determines ventral and dorsal telencephalic neuron types from human embryonic stem cells. *Development* **136**, 4055–4063 (2009).
26. Wen, X. *et al.* Kinetics of hedgehog-dependent full-length gli3 accumulation in primary cilia and subsequent degradation. *Mol. Cell Biol.* **30**, 1910–1922 (2010).
27. Joksimovic, M. *et al.* Wnt antagonism of shh facilitates midbrain floor plate neurogenesis. *Nat. Neurosci.* **12**, 125–131 (2009).
28. Menuet, A., Alunni, A., Joly, J. S., Jeffery, W. R. & Rétaux, S. Expanded expression of sonic hedgehog in *Astyanax* cavefish: Multiple consequences on forebrain development and evolution. *Development* **134**, 845–855 (2007).
29. Pottin, K., Hinaux, H. & Rétaux, S. Restoring eye size in *Astyanax mexicanus* blind cavefish embryos through modulation of the shh and fgf8 forebrain organizing centers. *Development* **138**, 2467–2476 (2011).
30. Sylvester, J. B., Pottin, K. & Streelman, J. T. Integrated brain diversity along the early neuraxes. *Brain Behavior Evol.* **78**, 237–247 (2011).
31. O'Connell, L. A. & Hofmann, H. A. Evolution of a vertebrate social decision-making network. *Science* **336**, 1154–1157 (2012).
32. Stephan, H., Frahm, H. & Baron, G. New and revised data on volumes of brain structures in insectivores and primates. *Folia Primatologica* **35**, 1–29 (1981).
33. Fraser, G. J., Bloomquist, R. F. & Streelman, J. T. A periodic pattern generator for dental diversity. *BMC Biol.* **6**, 32 (2008).
34. Chen, J. K., Taipale, J., Young, K. E., Maiti, T. & Beachy, P. A. Small molecule modulation of smoothed activity. *Proc. Natl Acad. Sci. USA* **99**, 14071–14076 (2002).
35. Chen, B. *et al.* Small molecule-mediated disruption of Wnt-dependent signaling in tissue regeneration and cancer. *Nat. Chem. Biol.* **5**, 100–107 (2009).

Acknowledgements

We thank Gareth Fraser, Karen Pottin and three anonymous reviewers for their critical comments on previous drafts of this manuscript, Ashley Womble and Vicky Snowden for their technical support, and the US NSF (IOS 0922964 and IOS 1146275 to J.T.S.) for funding. C.H. is supported by the EU FP7 ZF-Health, the Wellcome Trust and the MRC.

Author contributions

J.B.S., C.H. and J.T.S. designed experiments. J.B.S., C.A.R., C.Y. and J.N.P. conducted experiments. J.B.S. generated all figures and tables. J.B.S. and J.T.S. wrote the manuscript.

Additional information

Competing financial interests: The authors declare no competing financial interests.

Reprints and permission information is available online at <http://npg.nature.com/reprintsandpermissions/>

How to cite this article: Sylvester, J. B. *et al.* Competing signals drive telencephalon diversity. *Nat. Commun.* **4**:1745 doi: 10.1038/ncomms2753 (2013).